

# A Modified Compact Bi-Directional UWB Tapered Slot Antenna with Double Band-Notch Characteristics

Zaid A. Abdul Hassain<sup>1</sup>, Adham R. Azeez<sup>2</sup>, Mustafa M. Ali<sup>3</sup>, and Taha A. Elwi<sup>4</sup>

<sup>1,3</sup>Department of Electrical Engineering, Mustansiriyah University, Baghdad-10047-Iraq

<sup>2</sup>Faculty of Engineering, Uruk University, Baghdad, Iraq

<sup>4</sup>Department of Communication Engineering, Almammon University College, Baghdad, Iraq

Email: Zaidasaad\_79@uomustansiriyah.edu.iq; Adham.r.azeez@ieec.org; mustafa\_mahdi@uomustansiriyah.edu.iq; Taelwi82@gmail.com

## Abstract

This research puts forward a design regarding a novel compact bi-directional UWB (1.9–12 GHz) tapered slot patch antenna that has dual band-notches characteristics within 3.4–3.9 GHz applicable for WiMax application and 5–6 GHz applicable for WLAN (IEEE 802.11a and HIPERLAN/2 systems). A parasitic quasi-trapezoidal shape single split ring resonator SRR is positioned to secure the first WiMax band-notch to minimize the electromagnetic interference occurring in WiMax band. A single circular complementary split-ring resonator (CSRR) is etched to secure the second band-notch. Simulated and measured results showed a good match, thereby signifying that the proposed antenna is an optimum candidate for UWB communication applications along with the design guidelines to employ the notch bands in the preferred frequency regions.

## 1. Introduction

In recent years, ultra-wideband (UWB) antennas have gained much popularity to facilitate high data rate, low power density ( $\leq -41\text{dBm/MHz}$ ), better communication security as well as provide a simple hardware configuration for the antenna to be used in practical applications [1]. The imaging system integrated with UWB technology offers higher resolution range as well as greater penetration depth inside the materials [2–4]. The UWB frequency region from 3.1 to 10.6 GHz was assigned for the US Federal Communications Commission (FCC) for use in commercial applications. Many researchers have broadly presented tapered slots such as Vivaldi antenna (VA) [5–7] as an UWB antenna because of the associated low profile, wide bandwidth, high gain, good time-domain characteristics, as well as symmetric end-fire radiation pattern for both H-and E-planes.

Several modified VA structures have been presented as well as studied in a bid to continue with good VA performance and decrease antenna size. The authors in [8] put forward a modified improved radiation VA that was based on choke slots as well as regular slots edge with a loaded lens. In [9], miniaturized version of AV antenna that had a tapered slot edge was presented rather than using a rectangular slot to fully utilize the radiating patch area. In [10], a tiny AV

antenna that had good time-domain properties was presented. However, at low frequencies, directivity and antenna gain were low. The authors in [11] put forward a modified AV antenna that was based on a periodic slit edge geared with trapezoidal shaped dielectric lens and miniaturized size for extension of the low-frequency end and improve antenna gain during both high and low frequencies. In [12], an elliptically tapered AV antenna that contained comb-shaped slits, as well as curved inner edges near the bottom and top radiators, was put forward. The extension of the low-frequency band was done until 1.65 GHz to get the low-frequency high gain (9 dB at 2 GHz). In [13], an exponential slots edge AVA to improve the radiation and gain enhancement.

In this research work, a new modified, bi-directional tapered slot antenna with miniaturized size along with UWB features was proposed. Dual band-notch was associated with the antenna, in the range 3.4–3.9 GHz suitable for WiMax application and 5–6 GHz suitable for WLAN (IEEE 802.11a and HIPERLAN/2 systems).

## 2. Antenna Design

### 2.1. Design without band-notch

First, we present the basic antenna, lacking band-notch, which completely covers the UWB band. Fig. 1 shows the design of the put forward bi-directional tapered slot antenna, which includes two radiation tapered slot patches that are symmetrical. The printing of the antenna is done on the FR4 substrate material with 1.5 mm thickness and dielectric constant  $\epsilon_r = 4.4$ . The size of the substrate was found to be  $45 \times 55 \text{ mm}^2$ , which represents half the wavelength. A  $50 \Omega$  coplanar waveguide fed line was linked to the antenna. The following exponential curves represent the inner and outer radiation flares edges [14]:

$$y = C_1 e^{0rx} + C_2 \quad \dots (1)$$

$$C_1 = \frac{y_2 - y_1}{e^{0rx_2} - e^{0rx_1}} \quad \dots (2)$$

$$C_2 = \frac{y_1 e^{0rx_2} - y_2 e^{0rx_1}}{e^{0rx_2} - e^{0rx_1}} \quad \dots (3)$$

Here, determination of inner  $C_1$ ,  $C_2$  is done by  $O_r$  (opening Rate).

Table 1 presents the put forward optimal parameters associated with the antenna. The finite-element method is employed to simulate the antenna by making use of the High Frequency Structure Simulator Ansoft HFSS 13 software [16].

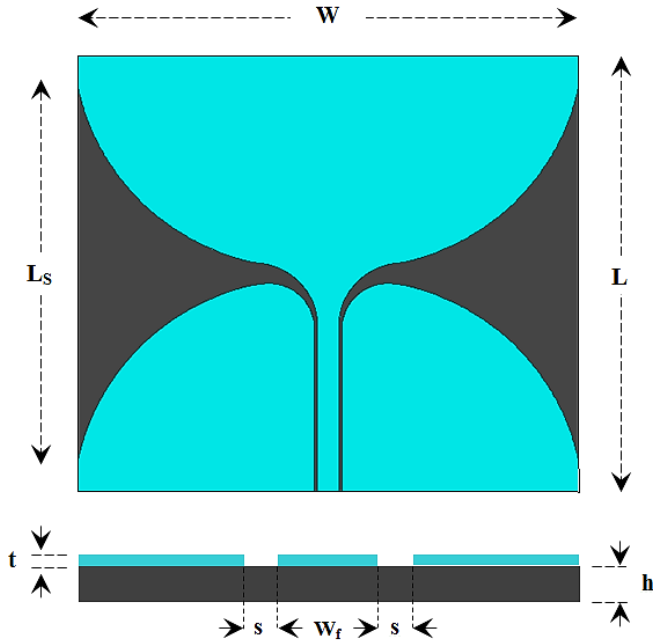


Figure 1: Proposed bi-directional antenna.

Table 1: Proposed antenna optimal parameters.

Parameters	L	W	Ls	h	t	Wf	s
Value (mm)	48	55	40.92	1.5	0.018	2.4	0.29

Fig. 2 presents the simulation  $S_{11}$  variation occurring for the modified bi-directional tapered slot antenna with UWB. The antenna encompasses the frequency band from 1.9 GHz up to 12 GHz.

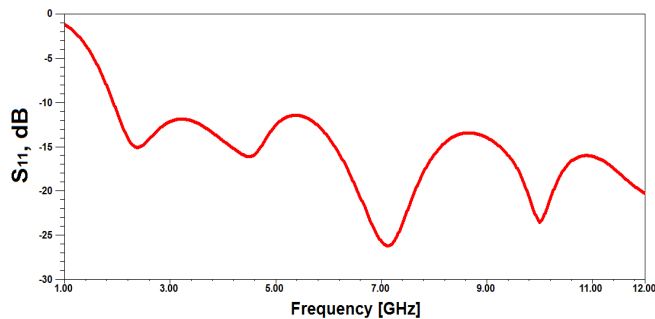


Figure 2: Simulated  $S_{11}$  of the proposed UWB antenna.

## 2.2. Single band-notch design

This section explains the design pertaining to single band-notch UWB antenna. A single parasitic SRR is introduced to minimize the electromagnetic interference found in the WiMAX frequency band (3.4–3.9 GHz) as displayed in Fig. 3. The SRR is placed strategically at a distance of 0.4 mm from the substrate edge to satisfy 3.5 GHz. The optimal parasitic SRR parameters are shown in Table 2. Fig. 4 presents the  $S_{11}$  variation that has been simulated. At  $f=3.67$  GHz, a high band-notch of  $-5$  dB was centered, which was extended from 3.44 to 3.9 GHz. Fig. 5 shows the simulated current distribution with regards to the radiating patch pertaining to the proposed antenna with a notched frequency of 3.67 GHz, which allows understanding the phenomenon responsible for this band-notch performance. For the current concentrates primarily on the parasitic SRR, the antenna impedance was seen to alter at this frequency because of the proposed structure's band-notched characteristics. Therefore, the suggested structure provides UWB characteristics that prevent any interference with the WiMAX.

Table 2: Parasitic SRR optimal parameters

Parameters	a	b	c	d	e	f	g
Value (mm)	7.1	3.6	2.59	2.31	2.4	4	0.4

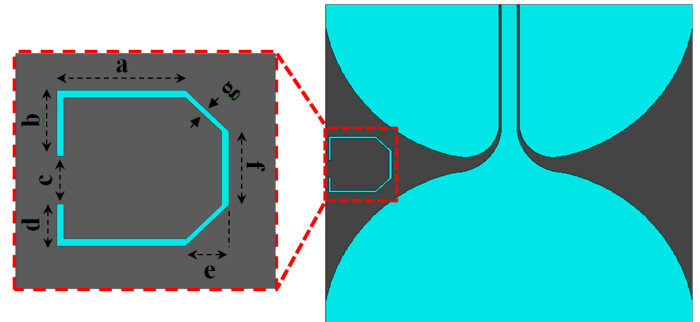


Figure 3: Proposed bi-directional antenna with single band-notch.

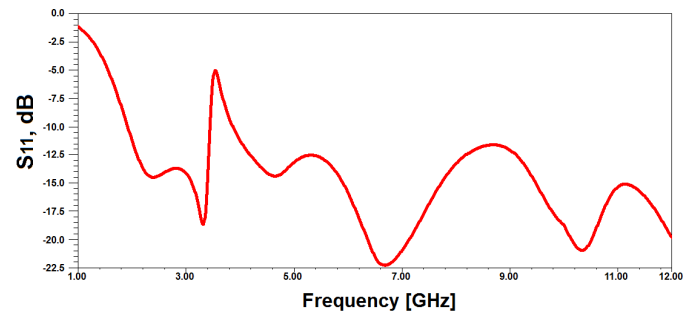


Figure 4: Simulated  $S_{11}$  of the proposed single band-notch antenna.

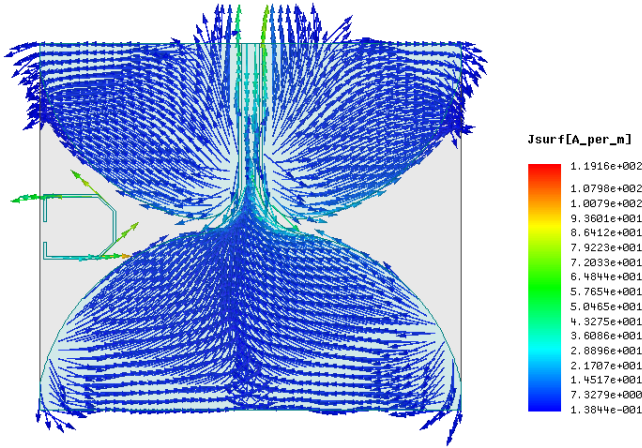


Figure 5: Surface current distribution at  $f=3.67$  GHz of single band-notch proposed antenna.

### 2.3. Dual band-notch design

For numerous applications of UWB, it is necessary that an UWB antenna is designed in a way that there is no electromagnetic interference with the WLAN band. Therefore, dual band-notched needs to be designed that can satisfy WLAN and WiMAX bands at the same time [15]. At a distance  $d_2$  away from the patch center, from the radiating patch, etching out of a single circular complementary split ring resonator (CSRR) is done. The final design regarding the suggested dual band-notch antenna is shown in Fig. 6. At  $f_{notch}=5.5$  GHz, tuning of the CSRR's length  $L$  is done by employing as [15]:

$$L = \frac{c}{2 f_{notch} \epsilon_{eff}} \quad \dots (4)$$

Where  $L$  denotes the CSRR length,  $\epsilon_{eff}$  represents the effective dielectric constant, which can be given as [15]:

$$\epsilon_{eff} = \frac{\epsilon_r + 1}{2} + \frac{\epsilon_r - 1}{2} \left[ 1 + \frac{12h}{W} \right]^{-\frac{1}{2}} \quad \dots (5)$$

Where  $\epsilon_r$  is relative permittivity,  $h$  is dielectric substrate thickness, and  $W$  is conductor width.

The simulated  $S_{11}$  variation is presented in Fig. 7. At  $f=5.5$  GHz, WLAN band-notch of  $-5$  dB was centered, which was extended from 5 to 6 GHz. As shown in Fig. 8, at a notched frequency of 5.5 GHz, a simulated surface current distribution is presented for the proposed antenna's radiating patch. For the current concentrates mostly on the inner and outer edges of the CSRR, it was seen that at this frequency, there is a change in the antenna impedance because of the proposed structure's band-notched characteristics. Therefore, UWB characteristics are provided by the proposed structure with no interference in the WLAN and WiMAX.

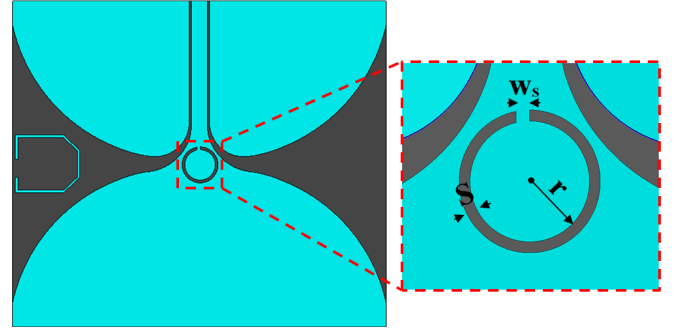


Figure 6: Proposed bi-directional antenna with dual-band notch characteristics.

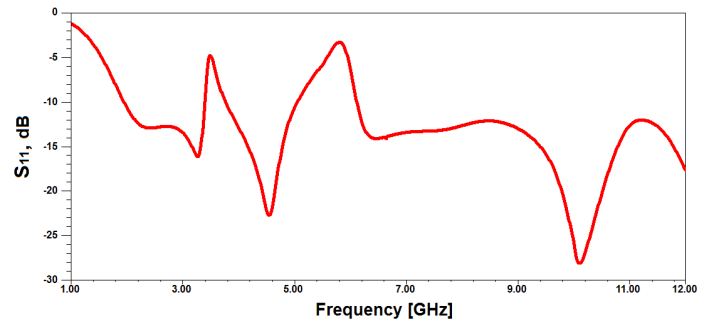


Figure 7: Simulated  $S_{11}$  of the proposed dual band-notch antenna.

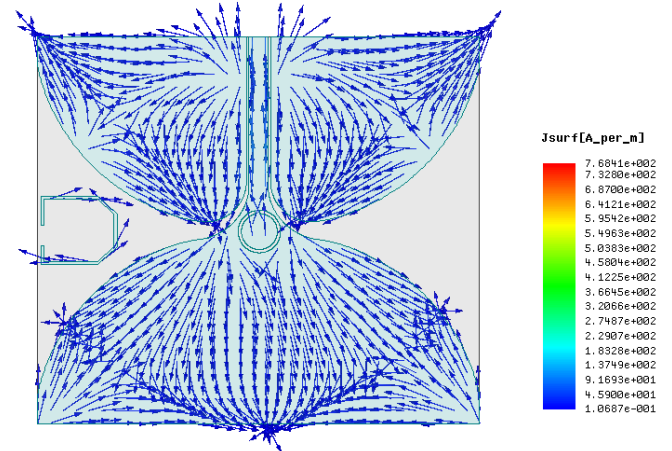


Figure 8: Surface current distribution at  $f=5.5$ GHz of the dual band-notch proposed antenna.

### 3. Radiation pattern and gain

This section describes the radiation pattern pertaining to the put forward dual band-notch UWB antenna. Fig. 9 presents the simulated far-field radiation pattern relating to the put forward antenna at frequencies of 4.5, 6.77 and 10 GHz pertaining to two principal planes, H- and E-planes. The 3D radiation plot is presented in Fig. 10. It can be said that end-fire characteristics are associated with the proposed antenna, which was found to be almost stable in the UWB frequency band.

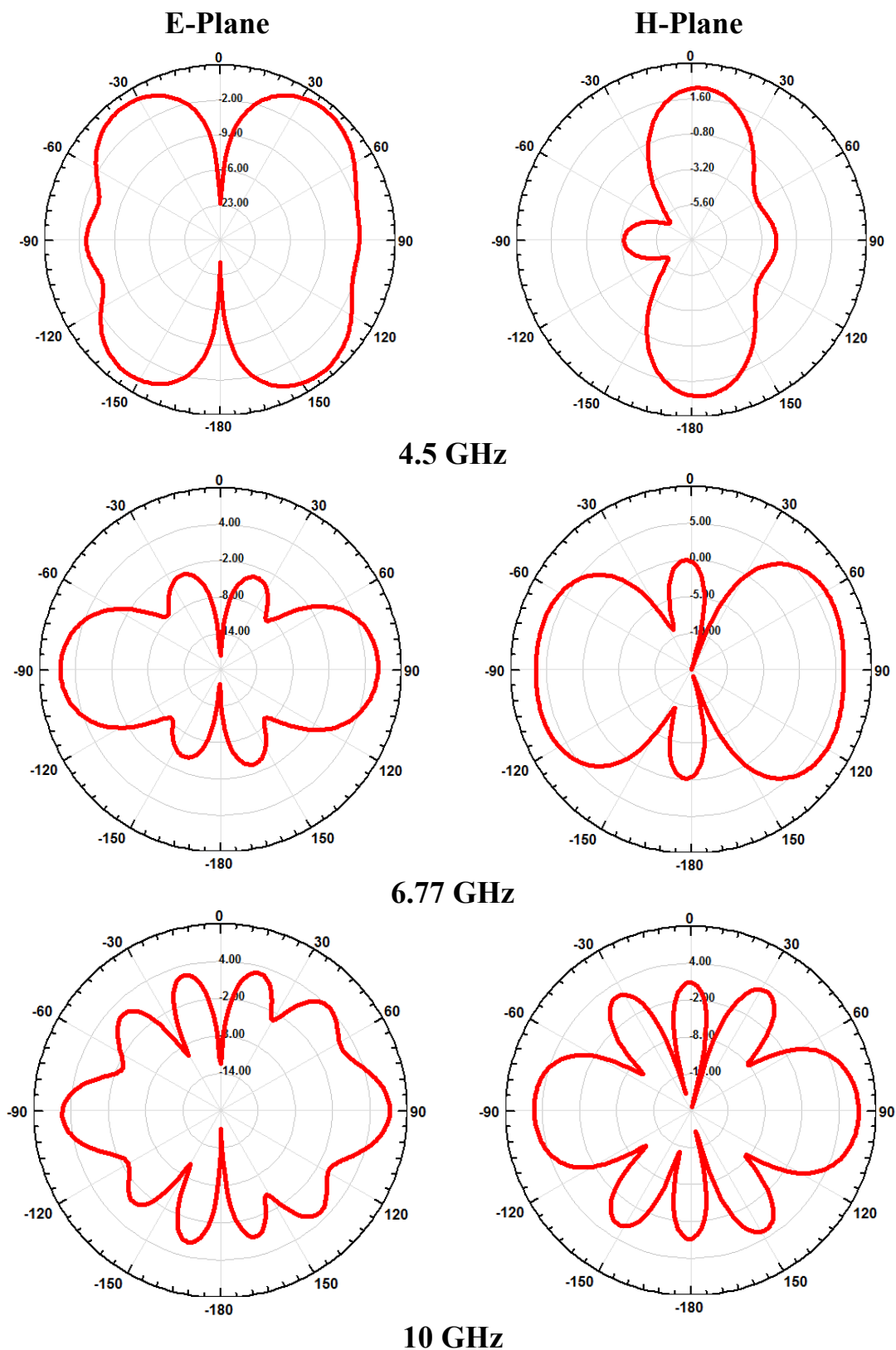


Figure 9: Simulated radiation patterns for the proposed antenna for the two principal planes (E-plane & H-plane), at three different operating frequencies.



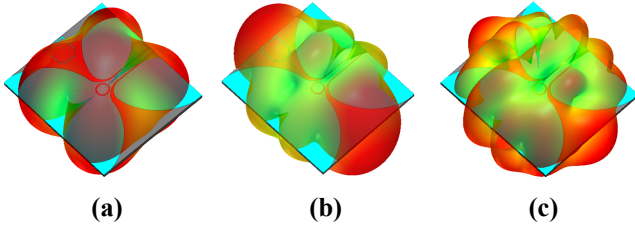


Figure 10: Simulated 3D radiation patterns for the proposed antenna at the frequencies: (a)  $f=4.5\text{GHz}$ , (b)  $f=6.77\text{ GHz}$  and (c)  $f=10\text{ GHz}$ .

#### 4. Experimental measurement

Fig. 11 shows the proposed dual band-notch antenna prototype. The proposed antenna is fabricated by using LPKF ProtoMat S100. The Anritsu Wiltron MS4642B Vector Network Analyzer was employed for the measurement. The measurement setup employed to characterize the proposed antenna is presented in Fig. 12.

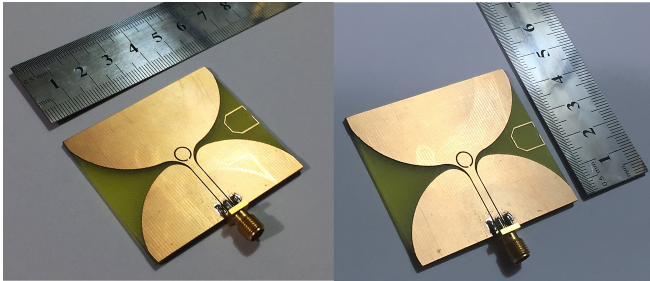


Figure 11: Dual band-notch antenna prototype



Figure 12: Measurement setup for the dual-band notch antenna.

With regards to  $S_{11}$ , the dual-band notch antenna structure's measurement and simulation results, as presented in Fig. 13, were compared. A good agreement could be established with a minor difference between the results. Such difference could be due to soldering defect, SMA mismatch, substrate and copper losses and certain error in the fabricating process.

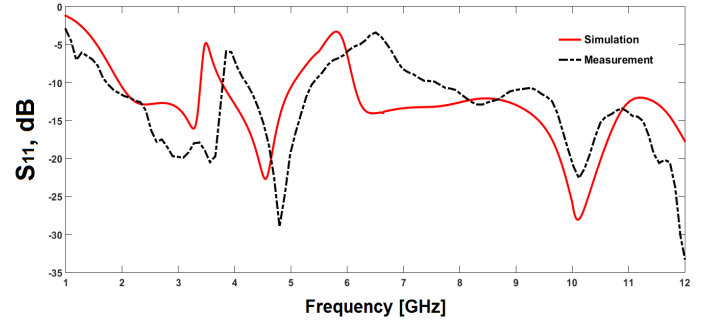


Figure 13: Measured and simulated  $S_{11}$  of the proposed dual band-notch antenna.

#### 5. Conclusion

This paper describes a new compact UWB (1.9–10.6 GHz) bi-directional tapered slot antenna that possesses dual and single band rejection properties. Two approaches were put forward pertaining to UWB band-notched design. With the help of single parasitic SRR that is trapezoidal, we presented the first band-notch. Based on this structure, high band notch could be obtained with about 5 dB at  $f=3.67\text{ GHz}$ . The second WLAN band-reject is obtained at  $f=5.5\text{ GHz}$  via a single circular CSRR etched out from the radiating patch. Therefore, UWB characteristics were found with the put forward structure with no interference seen in the WLAN and WiMAX. A good agreement was established between simulated and measured results, which suggest that this antenna is optimum for operating in imaging and UWB communications.

#### Acknowledgements

The authors would like to thank Mustansiriyah University ([www.uomustansiriyah.edu.iq](http://www.uomustansiriyah.edu.iq)) Baghdad-Iraq for its support in the present work.

#### References

- [1] Fontana, R. L., "Recent system applications of short-pulse ultra-wideband (UWB) technology," *IEEE Trans. MTT*, vol. 52, no. 9, pp. 2087-2104, 2004.
- [2] M. Moosazadeh and S. Kharkovsky, "Design of ultra-wideband antipodal Vivaldi antenna for microwave imaging applications," in *Proc. IEEE Int. Conf. Ubiquitous Wireless Broadband (ICUWB)*, pp. 1-4, 2015.
- [3] M. Moosazadeh and S. Kharkovsky, "Development of the antipodal Vivaldi antenna for detection of cracks inside concrete members," *Microw. Opt. Technol. Lett.*, vol. 57, no. 7, pp. 1573-1578, 2015.
- [4] Alexandre M. de Oliveira, João F. Justo, Marcelo B. Perotoni, Sérgio T. Kofuji, Alfredo G. Neto, Regis C. Bueno, and Henri Baudrand, "A high directive Koch

- fractal Vivaldi antenna design for medical near-field microwave imaging applications," *Microwave and Optical Technology Letters*, vol. 59, no. 2, February 2017.
- [5] Bourqui, J., M. Okoniewski, and E. C. Fear, "Balanced antipodal Vivaldi antenna with dielectric director for near-field microwave imaging," *IEEE Trans. Antennas Propag.*, vol. 58, no. 7, pp. 2318-2326, 2010.
- [6] Abbosh, A. M., "Miniaturized microstrip-fed tapered slot antenna with ultrawideband performance," *IEEE Antennas and Wireless Propagat. Lett.*, vol. 8, pp. 690-692, 2009.
- [7] Bai, J. , S. Y. Shi, and D. W. Prather, "Modified compact antipodal Vivaldi antenna for 4-50 GHz UWB application," *IEEE Trans. Microwave Theory Tech.*, vol. 59, no. 4, pp.1051- 1057, 2011.
- [8] Teni, G. , N. Zhang, J. H. Qiu, and P. Y. Zhang, "Research on a novel miniaturized antipodal Vivaldi antenna with improved radiation," *IEEE Antennas and Wireless Propagat. Lett.*, vol. 12, pp. 417-420, 2013.
- [9] Peng Fei, Yong-Chang Jiao, Wei Hu and, Fu-Shun Zhang, "A Miniaturized Antipodal Vivaldi Antenna With Improved Radiation Characteristics," *IEEE Antennas and Wireless Propagation Letters*, vol. 10, pp. 127-130, 2011.
- [10] Hood, A., Z. T. Karacolak, and E. Topsakal, "A small antipodal Vivaldi antenna for ultrawide-band applications," *IEEE Antennas and Wireless Propagat. Lett.*, vol. 7, pp. 656-660, 2008.
- [11] M. Moosazadeh and S. Kharkovsky, "A compact high-gain and front-to-back ratio elliptically tapered antipodal Vivaldi antenna with trapezoid-shaped dielectric lens," *IEEE Antennas Wireless Propag. Lett.*, vol. 15, pp. 552-555, 2016.
- [12] M. Moosazadeh, S. Kharkovsky, and J.T. Case, "Microwave and millimeter wave antipodal Vivaldi antenna with trapezoid-shaped dielectric lens for imaging of construction materials," *IET Microw. Antennas Propag.*, vol. 10, no. 3, pp. 301-309, 2016.
- [13] M. De Oliveira, B. Perotoni, T. Kofuji, and F. Justo, "A Palm Tree Antipodal Vivaldi Antenna with Exponential Slot Edge for Improved Radiation Pattern," *IEEE Antennas and Wireless Propagation Letters*, vol. 14, pp. 1334 - 1337, February 2015.
- [14] Josef Nevrl'y, "Design of Vivaldi Antenna", Diploma Thesis Czech Technical University, Prague Czech Republic, 2007.
- [15] D. Sarkar, K. Srivastava, and K. Saurav, "A Compact Microstrip-Fed Triple Band-Notched UWB Monopole Antenna", *IEEE Antennas and Wireless Propagation Letters*, vol. 13, 2014.
- [16] Ansoft HFSS [Online]. Available: <http://www.ansoft.com>.